Journal of Materials Chemistry B

Accepted Manuscript

ROYAL SOCIETY OF CHEMISTRY

www.rsc.org/materialsB

Journal of Materials Chemistry B

ARTICLE

Double Hydrophilic Polyphosphoester Containing Copolymers as Efficient Templating Agents for Calcium Carbonate Microparticles

Received 00th January 20xx,
Accepted 00th January 20xx

DOI: 10.1039/x0xx00000x

www.rsc.org/

Ergul Yilmax Zeynep[£§], Debuigne Antoine[£], Calvignac Brice[§], Boury Frank[§] and Jerome Christine*[,£]

Abstract. The use calcium carbonate ($CaCO_3$) microparticles is becoming more and more attractive in many fields especially for biomedical applications for which fine tuning of size, morphology and crystalline form of $CaCO_3$ particles is crucial. Although some structuring compounds, like hyaluronic acid, give satisfying results, the control of the particle structure still has to be improved. To this end, we evaluated the $CaCO_3$ structuring capacity of novel well-defined double hydrophilic block copolymers composed of poly(ethylene oxide) and of a polyphosphoester segment with affinity for calcium like poly(phosphotriester)s bearing pendant carboxylic acids or poly(phosphodiester)s with a negatively charged oxygen atom on each repeating monomer unit. These copolymers were synthesized by combination of organocatalyzed ring opening polymerization, thiol-yne click chemistry and protection/deprotection methods. The formulation of $CaCO_3$ particles was then performed in the presence of these block copolymers (*i*) by the classical chemical pathway involving $CaCl_2$ and Na_2CO_3 and (*ii*) by a process based on the supercritical carbon dioxide ($scCO_2$) technology in which CO_3^{2-} ions are generated in aqueous media and react with Ca^{2+} ions. Porous $CaCO_3$ microspheres composed of vaterite nanocrystals were obtained. Moreover, a clear dependence of the particle size on the structure of the templating agent was emphasized. In this work, we show that the use of the supercritical process and the substitution of the hyaluronic acid for the carboxylic acid containing copolymer allow to decrease the size of the $CaCO_3$ particles by a factor 6 (~1.5 µm) while preventing their aggregation.

Introduction

Nowadays, sustained drug delivery systems (DDS) involving purposely designed particles are gaining increasing importance for the human therapy such as cancer[1,2], bowel diseases[3,4], infectious diseases (tuberculosis)[5] and skin diseases[6], and for regenerative medicine such as bone cartilage[7], central nervous system[8], Parkinson diseases[9–11], Huntington diseases[12].The latter often requires biodegradable and biocompatible materials that allow the safe retention as well as controlled delivery of the drug, a better bioavailability and reduction of adverse effects. In this respect, calcium carbonate particles are safe, biocompatible and biodegradable microcontainers that can fulfill such functions. These inorganic carriers have excellent properties such as low density, high specific surface area and porosity allowing efficient drug encapsulation and release.[13–16] Moreover, their ease of preparation and low price make $CaCO_3$ particles very attractive for protein[17–22], drug[16,23–27], and gene[28,29] delivery.

$CaCO_3$ particles exist in three anhydrous polymorphs: calcite, aragonite and vaterite.[30–33] By far, the last crystalline form is the most interesting for the drug delivery applications because it exhibits a porous structure favourable to the encapsulation of therapeutic compounds.[23,34,35] Vaterite can easily be obtained in water by mixing aqueous calcium salt and carbonate solutions.[18,26] (Figure 1, upper part) The formulation of $CaCO_3$ particles often requires a templating agent able to control the particles size, shape and porosity. Double hydrophilic block copolymers (DHBCs) is a very efficient class of templating agent for controlling the crystallization of $CaCO_3$ particles.[36-44] They are composed of one hydrophilic segment which binds the calcium ions, provides sites of nucleation and controls the $CaCO_3$ crystal growth, associated to a second hydrosoluble block which ensures the steric stabilization of the growing crystals under high-ionic-strength condition. While PEO is almost invariably chosen as stabilizing block, several segments with alkaline earth ions binding capacities have been tested including poly(acrylic acid) (PAA), poly(methacrylic acid) (PMAA), polyanionic phosphate functionalized block[40], polyglycidol segments converted into ionic blocks containing carboxylic, sulfonic, or phosphoric acid groups.[42] As a result, $CaCO_3$ particles were produced with a wide variety of size and morphologies including spherical, hollow shape and many others. Interestingly, the templating capacity of phosphoric acid containing copolymers was found superior to their carboxylic and sulfonic counterparts[42].

Recently, some of us have demonstrated the benefit of using supercritical carbon dioxide ($scCO_2$) for the synthesis of $CaCO_3$ particles in the vaterite form.[15,18,35,45] (Figure 1, lower part) $ScCO_2$ is well adapted to the formulation of materials dedicated to biomedical applications[46-51] and in particular to the synthesis of

[a,£] Center for Education and Research on Macromolecules (CERM), University of Liège (ULg),Chemistry Department, Sart Tilman, Building B6a-third floor, Liège, B-4000, Belgium
[b,§] INSERM U1066, Micro et Nanomédecines Biomimétiques, IBS, University of Angers, 4 rue Larrey, Cedex 9, Angers, 49933, France
[c,] *corresponding author: c.jerome@ulg.ac.be

$CaCO_3$ carriers, because this supercritical fluid is non-toxic, non-flammable and environmentally benign solvent.[18,49-52] In addition, its quite low critical conditions (T= 31.1°C and P = 73.8 bar) enable handling sensitive compounds such as drugs and therapeutic proteins.[46,48-51] Hyaluronic acid (HA), i.e. a biodegradable polysaccharide bearing carboxylic acid pendent groups, was used as templating agent for the synthesis of $CaCO_3$ particles in $scCO_2$ and was found essential for the production of well-defined micrometer sized porous $CaCO_3$.[14,15,18,35] Nevertheless, the search for new efficient templating agents able to adjust and further decrease the size of the $CaCO_3$ particles is still relevant today.

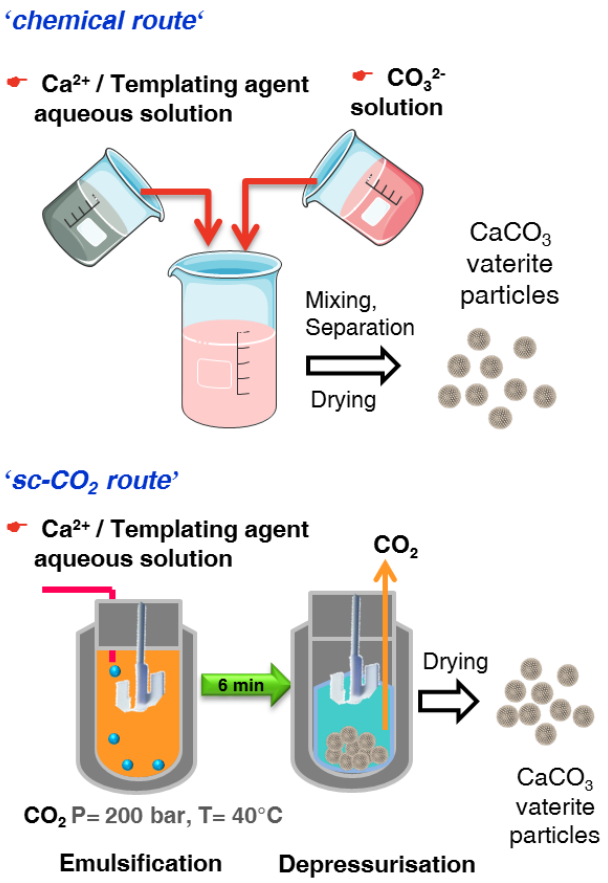

Figure 1. Illustration of the "chemical" and the "$scCO_2$" pathways for the synthesis of $CaCO_3$ vaterite particles.

In this study, we designed and explored the potential of a new class of biodegradable copolymers to template $CaCO_3$ particles. In particular, we focused on poly(phosphoester)s (PPEs) which keep the advantages of HA to be biodegradable and biocompatible materials. In contrast to HA, these synthetic polymers have structural similarities to nucleic and teichoic acids[53-55] and can be obtained with various and well-defined copolymer architectures and compositions.[56,57] As a consequence, PPE are nowadays already involved in many fields such as drug delivery[56,58-63], gene delivery[56,57,64], dental applications[65] and tissue engineering[65-67]. Above all, PPE derivatives might be excellent candidates for templating $CaCO_3$ particles because their phosphate degradation product could associate with calcium ions from the inorganic carrier and favour some reconstruction processes like bone regeneration. More particularly, we targeted double hydrophilic block copolymers composed of poly(ethylene oxide) (PEO) and of a PPE segment likely to have affinity for calcium ions like poly(phosphotriester)s bearing pendant carboxylic acids (scheme 1, structure 3) or poly(phosphodiester)s having a negatively charged oxygen atom on each repeating monomer unit (scheme 1, structure 6). Organocatalyzed Ring Opening Polymerization (ROP) of cyclic phospholane monomers,[53,68-71] thiol-yne click chemistry[70-73] and protection/deprotection methods were combined for preparing the desired well-defined block copolymers. Next, we evaluated the potential of these PPE containing copolymers for templating the $CaCO_3$ particles in water but also in water/$scCO_2$ mixture. The morphology of $CaCO_3$ particles was studied by scanning electron microscopy and X-ray analyses and compared to those produced with HA, the only previously reported polymer used for controlling the growth of $CaCO_3$ in $scCO_2$.

Experimental Part

Materials. 2-Chloro-2-oxo-1,3,2-dioxaphospholane (COP) (≥95%, Aldrich), dichloromethane (CH_2Cl_2) (Chem-lab), toluene (Chem-lab), tetrahydrofuran (THF) (Chem-lab), methanol (Sigma-Aldrich), n-pentane (extra pure, Acros), acetic acid (Fisher Scientific), diethylether (Et_2O) (Chem-lab), dimethylformamide (DMF) (Chem-lab), sodium thiophenolate (90%, Aldrich), 2,2-dimethoxy-2-phenylacetophenone (DMPA) (99%, Sigma-Aldrich), 3-mercaptopropionic acid (≥99%, Aldrich), poly(ethylene glycol) methyl ether (PEO-OH) (Aldrich), glycine (≥99%, Sigma), calcium hydroxide ($Ca(OH)_2$) (95%, Sigma–Aldrich), and hyaluronic acid (Streptococcus equi.) (Sigma), sodium carbonate (Na_2CO_3) (≥99.5%, Sigma-Aldrich), sodium chloride (NaCl) (≥97%, Fluka), sodium hydroxide (NaOH) (Fisher Chem) and calcium hydride (CaH_2) (90-95%, Aldrich), 3-butyn-1-ol (97%, Aldrich), 1-propen-3-ol (≥99%, Aldrich), triethylamine (TEA) (≥99%, Sigma-Aldrich) were used as received.1,8-diazobicyclo[5.4.0]undec-7-ene (DBU) (≥99%, Aldrich) were dried over calcium hydride at room temperature, following by distillation under reduced pressure just before use. Thiourea (TU) was synthesized according to the method described[74] and dried overnight under vacuum just before use. Ultrapure water (18 MΩ·cm) was acquired by means of a Milli-Q water filtration system, Millipore Corp. (St. Charles, MO). The photo-irradiation was carried out by a UV light source from OmniCure Series 2000 (200 W, 365 nm).

Characterization. ^1H and ^{31}P nuclear magnetic resonance (NMR) analyses were performed on a Bruker Advance 250 and 400 spectrometer (MHz) in deuterated chloroform ($CDCl_3$) and deuterium oxide (D_2O) at 25 °C in the FT mode. The MALDI-TOF spectrum was recorded with a UltrafleXtreme spectrometer (Bruker Daltonics, Germany) using 2,5-dihydroxybenzoic acid as a matrix and no additional cationating agent. Size exclusion chromatography (SEC) was carried out in DMF (flow rate 1 mL/min) at 40 °C using a Water 600 autosampler liquid chromatograph equipped with a differential refractometer index detector. Waters gel 5 µm (105,104, 500, and 100 Å) columns were calibrated with

polystyrene standards. Infrared spectra were recorded with a Perkin-Elmer FT-IR instrument (KBr). The size and morphology of the $CaCO_3$ microparticles were studied by scanning electron microscopy (SEM). After lyophilization, samples were sputtered with gold using a high vacuum metal evaporation coater MED 020 (Bal- Tec, Balzers, Lichtenstein) and observed using a scanning electron microscope (SEM. Jeol 6301F) at an operating voltage of 3 keV. The size and size distribution of $CaCO_3$ microparticles were determined by light scattering by using a particle size analyzer PSA in liquid medium (Malvern Mastersizer with hydro 2000S small volume sample dispersion unit, France). Microspheres were dispersed in phosphate buffer solution (PBS, pH: 7.4) and vortexed prior to every measurement. The laser diffusion intensity is recorded as a function of the angle of diffusion, and then application of the Fraunhofer diffraction and Mie scattering theories allows the size of the particles and their repartition in number to be obtained. All measurements were repeated three times with a stirring rate of 3500 rpm with no ultrasound. A Zetasizer 2000 (Malvern Instruments) operating at 150 mV and at room temperature was used to assess the zeta potential of the microparticles. The zeta cell was washed with ultrapure water between every measurement. The crystal structures of the $CaCO_3$ microspheres were characterized by X-ray diffraction. XRD analysis was carried out using an X-pert diffractometer (CuKα1α2 doublet, λ = 1.54056 Å, from 2θ = 10 to 70° in continuous mode with a step size of 0.07°).

Synthesis of butynyl phospholane (BYP) (monomer 1, scheme 1). A mixture of 3-butyn-1-ol (12.29 g, 176 mmol) and triethylamine (19.4 g, 192 mmol) in dry THF (150 ml) was cooled at 0°C. Then, a solution of 2-chloro-2-oxo-1,3,2-dioxaphospholane (COP) (25 g, 176 mmol) in dry THF (50 ml) was added dropwise under stirring to the reaction mixture ($[COP]_0/[TEA]_0/[3\text{-butyn-1-ol}]_0$ = 1/1.1/1). After complete addition, the stirring was pursued at 0 °C for 12 h. The resulting triethylamine hydrochloride salt was removed by filtration and the filtrate was concentrated by evaporation of the solvent. The residue was then purified by vacuum distillation to obtain a faint yellow and viscous liquid (110-120 °C, 10^{-4} Torr) with a yield of 24 %. ^{1}H NMR ($CDCl_3$, 250 MHz): 4.51 - 4.25 ppm (m, 4H, O-C$\underline{H_2}$-C$\underline{H_2}$-O), 4.29 - 4.00 ppm (m, 2H, O-C$\underline{H_2}$-CH$_2$-C), 2.51 ppm (t, 2H, O-CH$_2$-C$\underline{H_2}$-C), 1.99 ppm (s, 2H, O-CH$_2$-CH$_2$-C≡C$\underline{H}$). ^{31}P NMR ($CDCl_3$, 250 MHz): 17.8 ppm.

Synthesis of PEO-b-PBYP (copolymer 2, scheme 1) by ROP. TU (222 mg, 0.6 mmol) was placed in a round bottom flask and dried by three azeotropic distillations with toluene. BYP **1** (2.4 g, 13.6 mmol) and PEO-OH (Mn~5000 g mol^{-1}, 4.0 g, 0.80 mmol) were introduced in a second flask under an inert atmosphere, dried by three azeotropic distillations with toluene, solubilized in dry and degassed CH_2Cl_2 (6.4 mL) and transferred into the flask containing TU. Freshly distilled DBU (0.18 mL, 1.2 mmol) was then added to the solution ($[BYP]_0/[PEO\text{-}OH]_0/[DBU]_0/[TU]_0$ = 34/2/3/1.5, $M_{n\ th\ PBYP}$ = 3000 g mol^{-1}). The reaction medium was stirred at 0 °C for 5 minutes. The monomer conversion was evaluated to 83% based on the ^{31}P NMR spectrum. After removing the residual solvent under vacuum, the obtained copolymer was purified by precipitation in Et_2O. The obtained polymer was dissolved in methanol and dialyzed against methanol overnight in order to remove DBU and TU residues. After evaporation of methanol and drying under vacuum, PEO_{5k}-b-$PBYP_{2.3k}$ copolymer was collected and characterized by SEC, NMR and IR. ^{1}H NMR ($CDCl_3$, 250 MHz): 2.18-2.05 ppm (m, H, -O-CH$_2$-CH$_2$-C≡C$\underline{H}$), 2.7-2.3 ppm (m, 2H, O-CH$_2$-C$\underline{H_2}$-C≡CH), 3.38 ppm (s, 3H, CH$_2$-CH$_2$-O-C$\underline{H_3}$), 3.75-3.40 ppm (m, 8H, C$\underline{H_2}$-O-C$\underline{H_2}$-C$\underline{H_2}$-O-C$\underline{H_2}$), 4.7- 4.1 ppm (m, 4H, O-C$\underline{H_2}$-C$\underline{H_2}$-O, 4H, O-C$\underline{H_2}$-C$\underline{H_2}$-C). ^{31}P NMR ($CDCl_3$, 250 MHz): -1.76 ppm. $M_{n\ NMR\ PBYP}$ = 2300 g.mol^{-1}, $M_{n\ SEC\ PS}$ = 13000 g.mol^{-1}, Đ = 1.1. IR peak = 3463, 3290, 2888, 1637, 1466, 1343, 963, 810 cm^{-1}.

Synthesis of PEO-b-PBYPCOOH (copolymer 3, scheme 1) by thiol-yne reaction. PEO_{5k}-b-$PBYP_{2.3k}$ (0.30 g, 1.68 mmol of alkynes), 3-mercaptopropionic acid (1.76 g, 16.6 mmol) and DMPA (65.9 mg, 0.255 mmol) was dissolved in 10.0 mL of methanol and degassed by bubbling nitrogen for 10 min. The solution was then irradiated for 2 hours under UV (365 nm) at room temperature. The polymer was collected by precipitation into a pentane/diethyl ether mixture (3:1 ratio). After solubilisation in methanol, the copolymer was purified by dialysis (type of membrane cut off) against methanol overnight in order to remove the thiol residues and of the photoinitiator by-products. After drying under vacuum, the PEO-b-PBYPCOOH copolymer **3** was characterized by ^{1}H and ^{31}P. ^{1}H NMR (D_2O, 250 MHz): 3.37 ppm (s, 3H, CH$_2$-CH$_2$-O-C$\underline{H_3}$), 3.83-3.63 ppm (m, 8H, C$\underline{H_2}$-O-C$\underline{H_2}$-C$\underline{H_2}$-O-C$\underline{H_2}$), 1.80-2.05 ppm, 2.20-2.45 ppm (m, 2H, O-CH$_2$-C$\underline{H_2}$), 3.20-2.60 (m, 2H, C$\underline{H_2}$-COOH, 5H, CH$_2$-S-C$\underline{H_2}$-C$\underline{H}$-S-C$\underline{H_2}$), 4.53-4.20 (m, 2H, O-C$\underline{H_2}$-CH$_2$, 4H, O-C$\underline{H_2}$-C$\underline{H_2}$-O). ^{31}P NMR (D_2O, ppm, 250 MHz): -1.32 ppm. IR peak = 3550-3200, 2888, 1726, 1635, 1466, 1358, 1243, 1061, 1026, 984, 802 cm^{-1}.

Synthesis of Allyl Phospholane (AllP) (copolymer 4, scheme 1). 1-propen-3-ol (10.16 g, 0.175 mol) and triethylamine (17.71 g, 0.175 mol) were dissolved in dry THF (50 ml) and cooled to 0°C. A solution of COP (25 g, 0.175 mol) in dry THF (50 ml) was added dropwise under stirring ($[COP]_0/[TEA]_0/[1\text{-propen-3-ol}]_0$ = 1/1/1). After complete addition, the resulting mixture was stirred at 0°C for 5h. The triethylamine hydrochloride salt was removed by filtration and the filtrate was concentrated. The AllP was then purified by distillation under reduced pressure (80-90 °C, 10^{-4} Torr) with a yield of yield 27%. ^{1}H NMR ($CDCl_3$, 250 MHz); 4.97-4.46 ppm (m, 4H, O-C$\underline{H_2}$-C$\underline{H_2}$-O, 2H, O-C$\underline{H_2}$-CH=CH$_2$), 5.76-5.42 ppm (m, 2H, CH=C$\underline{H_2}$), 6.37-6.07 ppm (m, 1H, C$\underline{H}$=CH$_2$). ^{31}P NMR ($CDCl_3$, 250 MHz): 17.3 ppm.

Synthesis of PEO-b-PAllP (copolymer 5, scheme 1) by ROP. TU (740 mg, 2 mmol), AllP **4** (163 g mol^{-1} , 2 g, 12.2 mmol) and PEO-OH (Mn~5000 g mol^{-1}, 2.0 g, 0.40 mmol) were introduced in a flask under an inert atmosphere, dried by three azeotropic distillations with toluene and solubilized in dry and degassed toluene (8 mL). Freshly distilled DBU (0.3 mL, 2 mmol) was then added to the solution ($[AllP]_0/[PEO\text{-}OH]_0/[DBU]_0/[TU]_0$ = 61/2/10/10, $M_{n\ th\ AllP}$ = 5000 g mol^{-1}). The reaction medium was stirred at 0 °C for 5 minutes. The monomer conversion was evaluated to 80% based on the ^{31}P NMR spectrum. After removing the residual solvent under vacuum, the obtained copolymer was purified by precipitation in cold Et_2O. The obtained polymer was dissolved in methanol and dialyzed against methanol overnight in order to remove DBU and TU residues. After evaporation of methanol and drying under

vacuum, the PEO_{5k}-b-$PAllP_{2.5k}$ copolymer was collected and characterized by SEC and NMR. ^{1}H NMR ($CDCl_3$, 250 MHz) 4.44-4.09 ppm (m, 4H, O-C$\underline{H_2}$-C$\underline{H_2}$-O), 4.74-4.45 ppm (m, 2H, O-C$\underline{H_2}$-CH=CH_2), 5.52-5.13 ppm (m, 2H, CH=C$\underline{H_2}$), 6.17-5.70 ppm (m, 1H, C$\underline{H}$=CH_2), 3.38 ppm (s, 3H, CH_2-CH_2-O-C$\underline{H_3}$), 3.74-3.58 ppm (m, 8H, C$\underline{H_2}$-O-C$\underline{H_2}$-C$\underline{H_2}$-O-C$\underline{H_2}$), ^{31}P NMR ($CDCl_3$, 250 MHz): -1.36 ppm. $M_{n\ NMR\ PAllP}$ = 2500 g.mol^{-1}, $M_{n\ SEC\ PS}$ = 10800 g.mol^{-1}, Đ = 1.2.

Synthesis of PEO-b-PPDO$^-$ (copolymer 6, scheme 1) by deprotection of 5. PEO_{5k}-b-$PAllP_{2.5k}$ (0.50 g, 3 mmol) was stirred with 1.5 eq. of sodium thiophenolate (C_6H_5SNa) (0.6 g, 4.5 mmol) in a DMF/H_2O (50/50 v/v) mixture at room temperature for 3 h. The polymer was then collected by precipitation in cold diethyl ether. After solubilisation in DMF, the copolymer **6** was purified by dialysis (MWCO: 1 kDa) against Milli-Q water overnight. The PEO-b-PPDO$^-$ **6** was recovered by freeze-drying and characterized by ^{1}H and ^{31}P NMR in D_2O. ^{1}H NMR (D_2O, 250 MHz) 4.19-3.94 ppm (m, 4H, O-C$\underline{H_2}$-C$\underline{H_2}$-O), ^{31}P NMR (D_2O, 400 MHz): 0.4 ppm.

Preparation of $CaCO_3$ particles by the classical chemical route. According to previously reported procedure,[14,15,39] calcium chloride ($CaCl_2$) (1.6% w/v) was added to the glycine buffer (0.62 M NaCl and 0.62 M glycine), then the pH was adjusted to 10. Sodium carbonate (Na_2CO_3) (1.6% w/v) was added to the glycine buffer. Lastly, as an anionic organic template, HA (0.1% w/v) was added to the $CaCl_2$ solution. Precipitation of $CaCO_3$ was carried out by mixing an equal volume of calcium containing solution ($CaCl_2$) and carbonate containing solution (Na_2CO_3). After stirring for 5 min at room temperature, the obtained suspension was centrifuged for 10 minutes at 4000 rpm and washed twice when particles were unloaded. Finally $CaCO_3$ microparticles were recovered by freeze-drying.

The same procedure was repeated with PEO-b-PBYPCOOH **3** or PEO-b-PPDO$^-$ **6** instead of HA (0.1% w/v of copolymer in the calcium chloride solution).

Preparation of $CaCO_3$ particles by the $scCO_2$ process. The synthesis method used in this study was patented by Boury et al. [75] Calcium Chloride ($CaCl_2$) (1.6% w/v) was added to the glycine buffer (0.62 M NaCl and 0.62 M glycine), then the pH was adjusted to 10. HA (0.1% w/v) was added to the $CaCl_2$ solution. A stainless steel autoclave with a capacity of 500 mL (Separex, Champigneulles, France) was heated at 40.0±0.1 °C, and pressurized with CO_2 at 200±1 bar. Liquid CO_2 was pumped using a high-pressure membrane pump at 1 kg.h^{-1} (Milton Roy Europe, Pont Saint Pierre-France) and preheated using a heat exchanger before feeding the autoclave. The stirring speed was set at 1200 rpm, with a Teflon coated stirrer (Top-industrie, Vaux le Penil, France). Once, the equilibrium was reached (i.e. stable temperature and pressure), the previously prepared calcium aqueous solution (1.6 % w/v) was injected using an HPLC pump (Model 307, Gilson, Villiers le Bel, France) with a flow rate of 10 mL.min^{-1} and a nozzle with an inner diameter of 1 mm. Once injection is achieved, the final pressure was 240±5 bar and the stirring was maintained at 1200 rpm for 10 min. Then, the stirring was stopped and the autoclave was depressurized at a rate of 40–50 bar.min^{-1} prior to the lyophilization of the $CaCO_3$ microspheres.

The same procedure was repeated with PEO-b-PBYPCOOH **3** or PEO-b-PPDO$^-$ **6** instead of HA at (0.1% w/v of copolymer in the calcium chloride solution).

Results and Discussion

Synthesis of the $CaCO_3$ templating agents.

Two types of double hydrophilic copolymers were considered in this study for templating calcium carbonate particles. The first candidate consists in a diblock copolymer made of a PEO sequence associated to a poly(phosphotriester) block bearing carboxylic pendant groups which are known for their high capacity to complex calcium ions. In contrast to other previously reported PEO-*b*-PPE derivatives, this copolymer with acid groups cannot be produced by direct polymerization of the corresponding acid containing cyclic phospholane monomer. Indeed, such a monomer is extremely unstable and undergoes rapid degradation by ring opening reaction catalyzed by the carboxylic groups. For this reason, we considered to introduce the acid moieties along the polyphosphate backbone by post-modification of a PEO-b-PPE precursor. This two-step strategy is shown in Scheme 1 (route A). It consists in the ring opening polymerization (ROP) of butynyl phosphate monomer (BYP) **1** initiated from a PEO-OH monomethyl ether followed by addition of mercaptopropionic acid onto the pendant alkyne groups of the PEO-*b*-polybutynyl phosphate copolymer (PEO-*b*-PBYP) **2** by a photochemical thiol-yne click reaction inspired from a procedure by Wooley et al.[71] The synthesis of the desired PEO-b-PBYPCOOH **3** is presented and discussed hereafter.

Monomer **1** substituted by the alkynyl group (BYP) was obtained by coupling of 3-butyn-1-ol with 2-chloro-2-oxo-1,3,2-dioxaphospholane (COP) according to a well-established synthetic pathway for cyclic phospholane ester monomers [76-80]. The structure of the BYP **1** was confirmed by ^{1}H NMR spectrum (Figure 2). Indeed, chemical shifts and the relative intensities of the signals were in agreement with the values reported previously for this compound[70]. Furthermore, only one strong resonance appeared at 17.32 ppm in the ^{31}P NMR spectrum of BYP (Figure 2), which is typical of cyclic phospholane monomer and confirms the structure and purity of BYP monomer.

Journal of Materials Chemistry B

ARTICLE

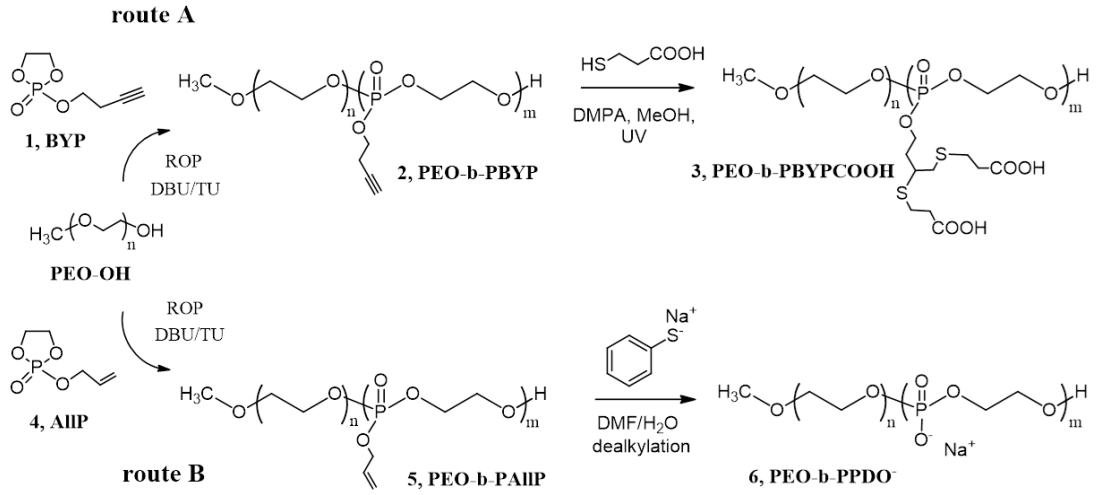

Scheme 1. General strategy for the synthesis of double hydrophilic copolymers with PEO as first block and poly(phosphotriester) with carboxylic acid pendant groups (route A) or anionic poly(phosphodiester)s (route B) as second block.

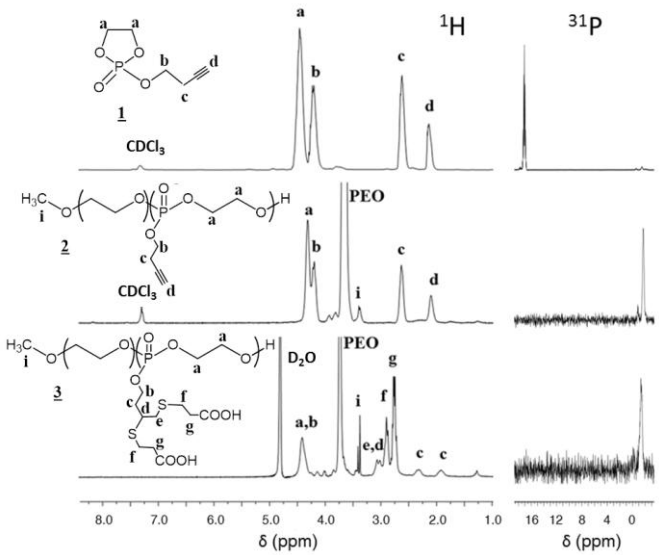

Figure 2. ^{1}H NMR and ^{31}P NMR spectra of the butynyl phosphate monomer **1** (upper spectrum, in $CDCl_3$), of PEO-*b*-PBYP **2** (middle spectrum, in $CDCl_3$) obtained by ROP and of PEO-*b*-PBYPCOOH **3** (lower spectrum, in D_2O) after thiol-yne reaction.

Polymerization of **1** was then initiated from a PEO-OH macroinitiator (M_n = 5000 g.mol^{-1}) in order to produce the PEO-b-PBYP **2**. The latter was performed by organocatalyzed-ROP in the presence of 1,8-diazabicyclo[5.4.0]undec-7-ene (DBU) and 1-1-[3,5-bis(trifluoromethyl)phenyl]-3-cyclohexyl-2-thiourea (TU) ($[DBU]_0/[TU]_0$ = 2). Substitution of organic compounds for metallic catalysts, like tin octoate, in the ROP prevents contamination of the final polymer by any metal traces that are incompatible with biomedical applications. Moreover, Clément et al. demonstrated the beneficial effect of using a DBU/TU mixture as catalysts for the polymerization of cyclic phospholanes on the polymerization kinetics and control.[53] As a matter of fact, DBU and TU system minimized the intra- and inter-molecular transesterification side reactions and is the most efficient catalytic method for this type of monomers.[53] Here, the ROP of BYP was carried out with both co-catalysts in dichloromethane at 0 °C. The BYP/PEO-OH molar ratio was adjusted to 17 in order to target a PBYP sequence of 3000 g.mol^{-1}. The conversion of **1** reached 83% after 10 minutes and the polymerization was stopped. After purification by precipitation in diethylether, the copolymer was analyzed by size exclusion chromatography (SEC). As shown in Figure S1, a clear shift of the SEC peak towards higher molar masses was observed, which proved the successful chain extension by ROP of BYP from the PEO-OH macroinitiator and the formation of the targeted PEO-*b*-PBYP. No residual PEO peak was left but a small peak was detected at lower elution volume compared to the major population. This higher molar mass peak might result from the polymerization of BYP initiated from traces of poly(ethylene oxide) having alcohol functions at both extremities of the chain (HO-PEO-OH) which contaminates the commercial PEO-OH[81] as evidenced by the MALDI-TOF spectrum (Figure S2). Nevertheless, well-defined PEO-*b*-

PBYP ($M_{n\ SEC\ DMF}$ = 13100 g.mol^{-1}, Đ = 1.1) was obtained. The actual molar mass and composition of the copolymer **2** was measured by ^{1}H NMR (Figure 2) considering the relative intensities of the PEO peak at 3.6 ppm and the signal corresponding to the propargylic protons **c** of the BYP units at 2.65 ppm. The molar mass of the PBYP block was evaluated to 2300 g.mol^{-1}, which is close to the theoretical prediction at 83% of conversion ($M_{n\ th}$ = 2500 g.mol^{-1}) and represents an average degree of polymerization (DP) of 13.

The post-modification of the pendant alkyne moieties of PEO_{5K}-*b*-$PBYP_{2.3K}$ was then performed by thiol-yne reaction in order to introduce carboxylic acids along the polyphosphate chains. Following a procedure adapted from Wooley et al.[71], mercaptopropionic acid (10 equ.) was reacted with alkyne in methanol under UV irradiation in the presence of catalytic amounts of 2,2-dimethoxy-2-phenylacetophenone (DMPA). After two hours, the irradiation was stopped and the copolymer was analyzed by IR (Figure S3) and ^{1}H NMR (Figure 2). The disappearance of C–H stretching band of the terminal alkyne at 3290 cm^{-1} and the apparition of an intense band at 1726 cm^{-1} typical of a carbonyl stretch C=O of a carboxylic acid confirmed the successful functionalization of the copolymer (Figure S3). In contrast to the starting PEO_{5K}-*b*-$PBYP_{2.3K}$ **2** that contains a hydrophobic PBYP block, the resulting PEO-b-PBYPCOOH **3** copolymer could easily be solubilized in water, which is another indication of the modification of the polymer, and in D_2O for ^{1}H NMR characterization (Figure 2). ^{1}H NMR evidenced the full consumption of the alkyne groups of **2** and the insertion of two carboxylic acid functions per BYP units in the copolymer **3**. Considering the near quantitative functionalization, the molar mass of **3** was calculated (PEO_{5K}-*b*-$PBYPCOO^-_{5K}$).

The second type of double hydrophilic copolymers prepared in this study consists in a PEO block linked to an anionic poly(phosphodiester) sequence bearing negatively charged oxygen atoms likely to complex calcium ions (copolymer **6** in scheme 1, PEO-b-PPDO$^-$). The general synthetic strategy (scheme 1, route B) relies on the ROP of 2-(prop-2-en-1-yloxy)-1,3,2-dioxaphospholane 2-oxide **4**, a cyclic phospholane monomer with an allyl moiety as side chain (AllP), followed by nucleophilic deprotection of the allyl group of PEO-*b*-poly(allyl phospholane) **5**. Compared to other strategies reported for the synthesis of poly(phosphodiester)s [68], the deprotection of the allyl group can be achieved under non acidic conditions, which prevents premature degradation of the poly(phosphate) chain.

First, prop-2-en-1-ol was esterified with 2-chloro-1,3,2-dioxaphospholane-2-oxide (COP) in the presence of triethylamine (TEA) leading to **4**, whose purity and structure were confirmed by ^{1}H NMR (Figure 3). Next, the metal free ROP of **4** was initiated from PEO-OH (5000 g.mol^{-1}) using the above mentioned DBU/TU catalytic system in toluene at 0 °C ([**4**]$_0$/[PEO-OH]$_0$/[DBU]$_0$/[TU]$_0$ = 30/1/5/5). The monomer conversion, calculated based on the relative intensity of monomer and polymer signal on the ^{31}P NMR spectrum (Figure 3), reached over 80 % within 10 minutes. SEC analysis proved the successful block copolymerization and formation of PEO-b-PAllP **5** ($M_{n\ SEC}$ = 10800 g/mol, Đ <1.2) (Figure S4). Again, the copolymer is contaminated by about 10% of a higher molar mass copolymer probably due to the presence of traces of bifunctional HO-PEO-OH in the commercial monomethylether PEO. The composition and average molar mass of **5** were determined by ^{1}H NMR (Figure 3) by comparison of the intensity of the signal corresponding to PEO at 3.65 ppm with the peak assigned to the allylic protons **b** of the PAllP block at 4.65 ppm ($M_{n\ PEO}$ = 5000 g.mol^{-1}, $M_{n\ NMR\ PallP}$ = 2500 g.mol^{-1}, $DP_{\ PAllP}$ = 16).

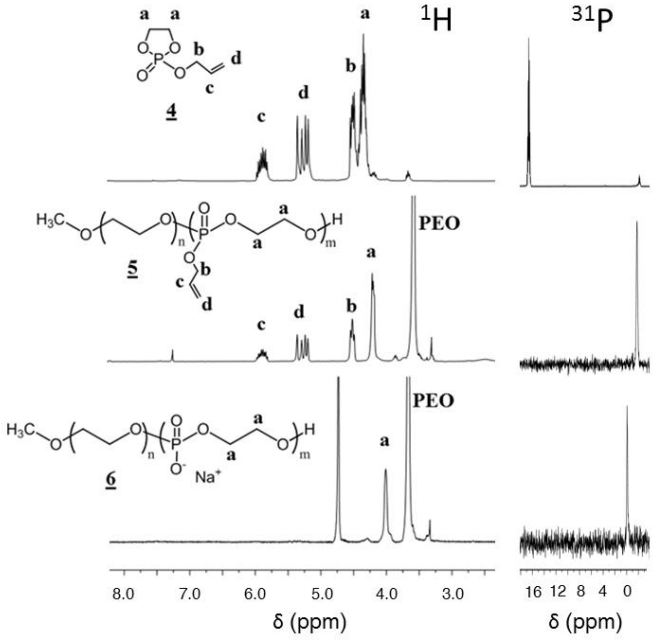

Figure 3. ^{1}H NMR and ^{31}P NMR spectra of the cyclic allyl phospholane monomer **4** (upper spectrum, in $CDCl_3$), of PEO-*b*-PAllP **5** (middle spectrum, in $CDCl_3$) obtained by ROP and of PEO-*b*-PPDO$^-$ **6** (lower spectrum, in D_2O) after deprotection.

In the last step, deprotection of PEO_{5K}-*b*-poly(allyl phospholane)$_{2.5K}$ into the negatively charged PEO-b-PPDO$^-$ **6** was carried out at room temperature in a DMF/water mixture with sodium benzenethiolate (C_6H_5SNa) (Scheme 1, route B). The ^{1}H NMR analysis in D_2O shown in Figure 3 demonstrates the quantitative removal of the allyl protective groups of **5**. Indeed, no signals of vinylic and allylic protons were found in the spectrum of **6** at 5.2 - 6.1 ppm and 4.58 ppm, respectively. At the same time, the signal corresponding to the protons of the -O-CH_2-CH_2-O- of the poly(phosphate) backbone were shifted from 4.3 ppm to 4.0 ppm compared to a native polymer. ^{31}P NMR of the PEO-b-PPDO$^-$ **6** shows only one single peak at 0.40 ppm (Figure 3), which proves that the deprotected poly(phosphodiester)-based copolymer is not contaminated by other phosphorous impurities and that no hydrolysis occurs during the deprotection step. Therefore, PEO_{5K}-b-$PPDO^-_{1.9K}$ having an average number of 16 negatively charged oxygen atoms per chain was successfully synthesized.

Calcium carbonate microparticles formation

The control of the size, the shape, and the crystal structure of the calcium carbonate particles are very important for tuning their properties for specific applications. Among the "crystal engineering" methods, macromolecules able to interact with

inorganic salts were used as templating agent during nucleation and growth of crystals[39]. For example, mixing calcium salt ($CaCl_2$) and carbonate (Na_2CO_3) aqueous solutions (called here the "chemical route") is a very popular pathway for the formation $CaCO_3$ particles.[19,22,39,82-84] In addition to glycine[85,86], the use of hyaluronic acid (HA), an anionic biopolymer, in the particles formulation allows directing the polymorphism of $CaCO_3$ into the vaterite form[15,18,87]. Under these conditions, spherical particles are formed with an average diameter of 1.5 µm as shown by Figure 4A. Nevertheless, the SEM image reveals rather important particles size dispersity and a tendency to aggregation.

Recently, some of us [14,15,18] developed a novel method for the production of $CaCO_3$ particles involving HA as templating agent and supercritical carbon dioxide which serves as source of carbonate ions (called here "$scCO_2$ process"). Typically, a $CaCl_2$ aqueous solution containing HA and buffered by glycine is injected into a reactor pressurized with CO_2 at 200±1 bars at 40±0.1 °C followed by depressurization at 40-50 bars.min^{-1} leading to $CaCO_3$ microparticles formation. After the injection of the basic solution in the autoclave, the fast diffusion of CO_2 molecules into the salt solution leads to the formation of ionic species such as HCO_3^- and CO_3^{2-}. The latter species react with Ca^{2+} ions and form the $CaCO_3$ particles with a spherical shape. In our set of experiments, we obtained also spherical microparticles with an average diameter of 8.5 µm (Figures 4D). It is shown that the particles formed in $scCO_2$ media are bigger but less aggregated. It has been shown previously that zeta potential of $CaCO_3$ particles produced with HA was more negative when formulated by $scCO_2$ route than in chemical route[18]. This could lead to better electrostatic repulsion and explain a beneficial effect on the level of aggregation of the particles (compare Figures 4A and 4D).

With these references in hands, the double hydrophilic copolymers PEO-b-PBYPCOOH **3** and PEO-b-PPDO$^-$ **6** were tested as a substitute of HA for the preparation of $CaCO_3$ microparticles in the chemical route and $scCO_2$ process. In this case, we expect that the PEO block will only slightly interact with the dissolved ions and ensure the water solubility whereas the charged polyphosphoester segment (PBYPCOO$^-$ or PPDO$^-$) will strongly interact with the inorganic salts and control the nucleation and growth of the crystal.

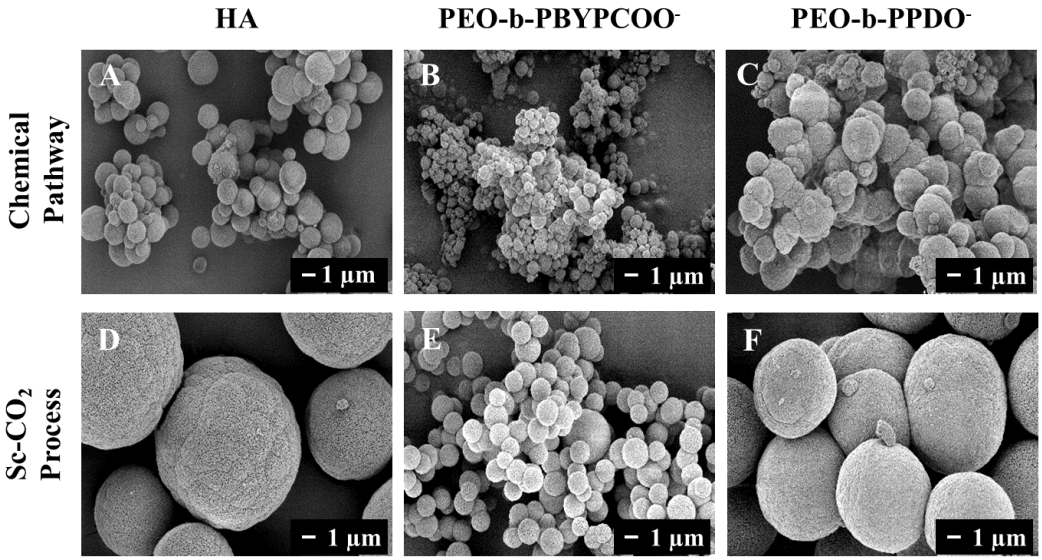

Figure 4. SEM observations of $CaCO_3$ particles prepared by chemical route (A-C) and $scCO_2$ process (D-F) in the presence of hyaluronic acid (A, D), PEO-b-PBYPCOOH **3** (B, E) or PEO-b-PPDO$^-$ **6** (C, F).

When mixing $CaCl_2$ and Na_2CO_3 according to the above mentioned chemical route in the presence of **3** and **6** in place of HA, micron-sized particles are formed and the SEM analyzes emphasized the crucial impact of the templating agent on the morphology of $CaCO_3$ particles (Figure 4B and 4C). Indeed, particles obtained in the presence of **6** are bigger (4 µm), poorly defined and largely aggregated. In contrast, using PEO-b-PBYPCOOH **3** in the formulation decreases the size of the particles down to 0.8 µm, which is significantly smaller than those obtained with HA. Unfortunately, in the latter case, aggregation of particles was also pronounced.

Then, formation of calcium carbonate by the $scCO_2$ process was tested with copolymers **3** and **6**. Particles formed in the presence of PEO-b-PPDO$^-$ **6** in $scCO_2$ are clearly better isolated from each other but also much more regular (Figure 4F) than those formed by the chemical route (Figure 4C). The average size of particles was larger according to the $scCO_2$ process (6.7 µm, Figure 4F), as it was the case for HA (compare Figures 4A and 4D). Overall, rather similar particles are formed with HA and PEO-b-PPDO$^-$ **6** in $scCO_2$. In contrast, PEO-b-PBYPCOOH **3** leads to much smaller particles (1.5 µm) in $scCO_2$ than HA (compare Figures 4E and 4D) while preventing aggregation of the particles. These size and size distribution evolutions were also confirmed by light scattering (LS) measurements (Figure S5 and Table S1) on the particles samples dispersed in phosphate buffer.

These observations clearly demonstrate the possibility to tune and reduce the size of the $CaCO_3$ particles by a factor 6 when using the copolymer **3** instead of the HA. Given the wide difference of structure between **3** and HA, it is difficult to point one specific structural parameter responsible for the difference in the $CaCO_3$ particle size. However, this size effect could be related to the

presence of the neutral PEO segment on **3** which could limit the growth of the microparticles. In addition, the high carboxylic acid density of the compound **3** as compared to HA might also favor the interaction of **3** with $CaCO_3$ nuclei and slow down their growth. Moreover, PEO-b-PBYPCOOH **3** is much more efficient than PEO-b-PPDO$^-$ **6** for templating the calcium carbonate particles most probably due to a higher calcium ion complexation ability and interaction with inorganic surfaces of carboxylic groups compared to the negatively charged phosphodiester moiety. Zeta potential of all the particles (Table S1) is clearly negative evidencing the presence of the stabilizing copolymers at their surface. The lower values obtained for the block-copolymers as compared to HA could reflect the presence of the neutral PEO segment partially screening the charges.

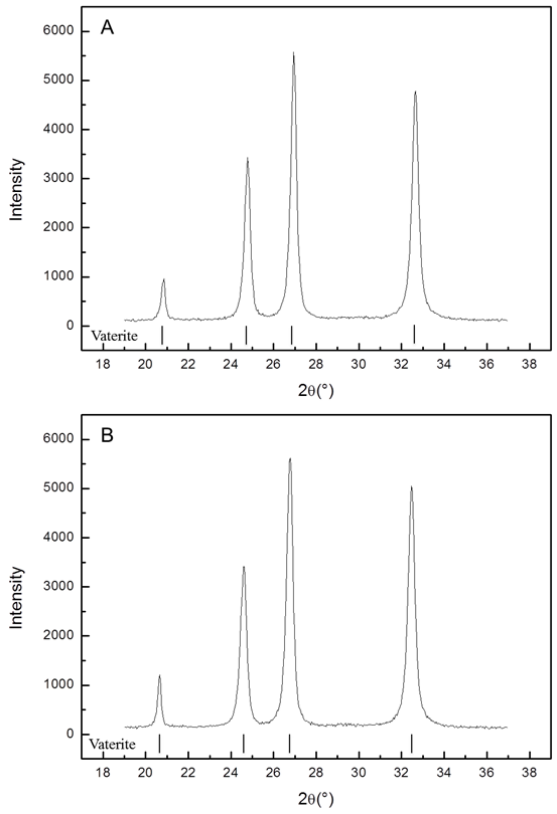

Figure 5. Structural analysis of XRD of the vaterite $CaCO_3$ particles prepared by the "$scCO_2$ route" in the presence of PEO-b-PBYPCOOH (A) or PEO-b-PPDO- (B). Bragg reflexions of the vaterite polymorph (ICSD 15879) are indicated with vertical markers below the profile.

XRD analysis of the particles prepared in CO_2 with copolymers **3** and **6** evidenced that $CaCO_3$ is in the vaterite form (Figure 5) as was the case for HA.[88] Based on the analysis of the broadening of the XRD peaks by the Debye-Sherrer equation, the size of the vaterite crystals that compose both types of microspheres is approximately 25±5 nm. The crystals size appears quite similar to those obtained with HA[88] showing that the templating polymer has few if any influence on the vaterite nanograins size. This observation is in line with the formation of vaterite nanocrystals mainly governed by the ionic strength, pressure and temperature of the medium that are comparable in all experiments.[88,89]

Close examination of cleaved microspheres by SEM evidenced a clear effect of the templating polymer on the internal morphology of the produced calcium carbonate particles (Figure 6A and 6B). Particles prepared in presence of PEO-b-PBYPCOOH are composed of individual aggregated and spherical nanograins and with a less compact structure than in presence of HA. This demonstrates the key role of the templating polymer on the packing of the vaterite nanograins to form the microsphere. Remarkably, the porous structure of the $CaCO_3$ particles prepared in $scCO_2$ with **3** exhibiting a central cavity (Figure 6B) could be of particular interest for applications involving the particle loading like drug delivery systems.

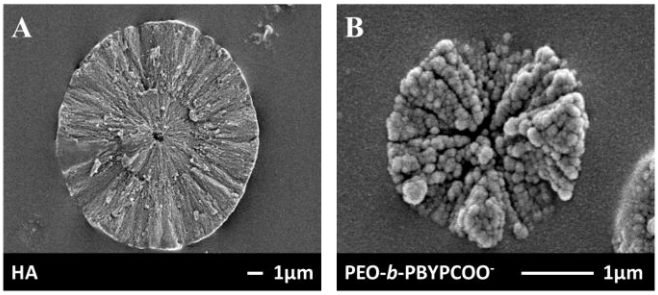

Figure 6. SEM images of broken $CaCO_3$ porous particles prepared in $scCO_2$ in the presence of HA (A) and PEO-b-PBYPCOOH **3** (B).

Conclusion

The formulation of $CaCO_3$ particles was performed in the presence of novel well-defined double hydrophilic copolymers containing a PEO segment associated to a poly(phosphotriester) block with pendant carboxylic moieties or to a negatively charged poly(phosphodiester). Two sets of conditions were evaluated, i.e. the classical chemical route involving $CaCl_2$ and Na_2CO_3 and a recently reported process based on the supercritical carbon dioxide technology using CO_2 as source of carbonate. Spherical $CaCO_3$ particles in the vaterite form were obtained in all cases but a dependence of the particle size on the structure of the templating agent was observed by SEM. Particles obtained with the acid containing copolymer PEO-b-PBYPCOOH **3** exhibit a low size dispersity and were 6 times smaller (1.5 µm) than those produced by HA. To the best of our knowledge, it is the smallest vaterite particles ever formulated in $scCO_2$. In contrast, rather similar particles were collected when using the poly(phosphodiester) derivative (PEO-b-PPDO$^-$) **6** and HA. The high density of carboxylic acids and the stronger calcium affinity of acid moieties compared to the negatively charged poly(phosphodiester) units most probably account for the excellent templating capacity of the PBYPCOOH containing copolymer. It is also worth noting that the level of particles aggregation was much lower with the $scCO_2$ formulation process compared to the classical procedure based on $CaCl_2$ and Na_2CO_3. The internal structure of the particles was also proved porous with an internal cavity in their center, which is of particular interest for encapsulation of biomolecules and delivery applications. These new poly(phosphate)-based templating agents notably pave the way to the design of inorganic drug carriers with tunable size and morphology, pointing the possibility to adjust and optimize their loading capacity and release profile.

Acknowledgements

The authors are grateful for the European financial support in the frame of the NanoFar program, an Erasmus Mundus Joint Doctorate (EMJD) program in nanomedicine and pharmaceutical innovation. They also thank the "National Funds for Scientific Research" (FRS-FNRS) and the Belgian Science Policy for financial support in the frame of the Interuniversity Attraction Poles Program (P7/05)–Functional Supramolecular Systems (FS2) for financial support. The authors thank also Dr. Thomas Beuvier from the Institut des Molécules et des Matériaux du Mans (Le Mans, France) for XRD analyses, M. R. Mallet of the SCIAM laboratory (Angers, France) for SEM analyses and M. J. Haler of the mass spectrometry laboratory (Prof. E. De Pauw, University of Liege, Belgium) for the MALDI-TOF.

Notes and references

1 J. Gong, R. Jaiswal, J.-M. Mathys, V. Combes, G. E. R. Grau and M. Bebawy, *Cancer Treat. Rev.*, 2012, **38**, 226–234.
2 Y. Sun, Y. Wang, C. Niu, E. M. Strohm, Y. Zheng, H. Ran, R. Huang, D. Zhou, Y. Gong, Z. Wang, D. Wang and M. C. Kolios, *Adv. Funct. Mater.*, 2014, **24**, 7674–7680.
3 C. Lautenschläger, C. Schmidt, D. Fischer and A. Stallmach, *Adv. Drug Deliv. Rev.*, 2014, **71**, 58–76.
4 E.-M. Collnot, H. Ali and C.-M. Lehr, *J. Control. Release*, 2012, **161**, 235–246.
5 S. Suarez, P. O'Hara, M. Kazantseva, C. E. Newcomer, R. Hopfer, D. N. Mcmurray and A. J. Hickey, *J. Antimicrob. Chemother.*, 2001, **48**, 431–434.
6 T. W. Prow, J. E. Grice, L. L. Lin, R. Faye, M. Butler, W. Becker, E. M. T. Wurm, C. Yoong, T. a Robertson, H. P. Soyer and M. S. Roberts, *Adv. Drug Deliv. Rev.*, 2011, **63**, 470–491.
7 E. Quinlan, A. López-Noriega, E. Thompson, H. M. Kelly, S. A. Cryan and F. J. O'Brien, *J. Control. Release*, 2014, **198**, 71–79.
8 S. M. Schindler, J. P. Little and A. Klegeris, *Biomed Res. Int.*, 2014, **2014**, 1–17.
9 C. Gujral, Y. Minagawa, K. Fujimoto, H. Kitano and T. Nakaji-Hirabayashi, *J. Control. release*, 2013, **168**, 307–316.
10 M. Shin, H. K. Kim and H. Lee, *Biotechnol. Prog.*, 2013, **30**, 215–223.
11 E. Garbayo, C. N. Montero-Menei, E. Ansorena, J. L. Lanciego, M. S. Aymerich and M. J. Blanco-Prieto, *J. Control. release*, 2009, **135**, 119–126.
12 S. Koennings, A. Sapin, T. Blunk, P. Menei and A. Goepferich, *J. Control. release*, 2007, **119**, 163–172.
13 Y. Zhang, *World J. Nano Sci. Eng.*, 2012, **02**, 25–31.
14 T. Beuvier, B. Calvignac, G. J.-R. Delcroix, M. K. Tran, S. Kodjikian, N. Delorme, J.-F. Bardeau, A. Gibaud and F. Boury, *J. Mater. Chem.*, 2011, **21**, 9757–9761.
15 M.-K. Tran, L. N. Hassani, B. Calvignac, T. Beuvier, F. Hindré and F. Boury, *J. Supercrit. Fluids*, 2013, **79**, 159–169.
16 D. Volodkin, *Adv. Colloid Interface Sci.*, 2014, **207**, 306–324.
17 M. Fujiwara, K. Shiokawa, M. Araki, N. Ashitaka, K. Morigaki, T. Kubota and Y. Nakahara, *Cryst. Growth Des.*, 2010, **10**, 4030–4037.
18 L. N. Hassani, F. Hindré, T. Beuvier, B. Calvignac, N. Lautram, A. Gibaud and F. Boury, *J. Mater. Chem. B*, 2013, **1**, 4011–4019.
19 A. I. Petrov, D. V Volodkin and G. B. Sukhorukov, *Biotechnol. Prog.*, 2005, **21**, 918–925.
20 S. Schmidt and D. Volodkin, *J. Mater. Chem. B*, 2013, **1**, 1210–1218.
21 D. V Volodkin, N. I. Larionova and G. B. Sukhorukov, *Biomacromolecules*, 2004, **5**, 1962–1972.
22 D. V Volodkin, A. I. Petrov, M. Prevot and G. B. Sukhorukov, *Langmuir*, 2004, **20**, 3398–3406.
23 Y. Svenskaya, B. Parakhonskiy, A. Haase, V. Atkin, E. Lukyanets, D. Gorin and R. Antolini, *Biophys. Chem.*, 2013, **182**, 11–15.
24 W. Wei, G. Hu, D. Yu, T. Mcleish, Z. Su and Z. Shen, *J. Am. Chem. Soc.*, 2008, **130**, 15808–15810.
25 Y. Zhang, P. Ma, Y. Wang, J. Du, Q. Zhou, Z. Zhu, X. Yang and J. Yuan, *World J. Nano Sci. Eng.*, 2012, **2**, 25–31.
26 M. Fujiwara, K. Shiokawa, T. Kubota and K. Morigaki, *Adv. Powder Technol.*, 2014, **25**, 1147–1154.
27 Y. Ueno, H. Futagawa, Y. Takagi, A. Ueno and Y. Mizushima, *J. Control. Release*, 2005, **103**, 93–98.
28 X. He, T. Liu, Y. Chen, D. Cheng, X. Li, Y. Xiao and Y. Feng, *Cancer Gene Ther.*, 2008, **15**, 193–202.
29 D. Zhao, C.-Q. Wang, R.-X. Zhuo and S.-X. Cheng, *Colloids Surf. B. Biointerfaces*, 2014, **118**, 111–116.
30 N. H. De Leeuw and S. C. Parker, *J. Phys. Chem.*, 1998, **102**, 2914–2922.
31 C. Y. Tai and F. Chen, *AIChE J.*, 1998, **44**, 1790–1798.
32 S. Ouhenia, D. Chateigner, M. A. Belkhir, E. Guilmeau and C. Krauss, *J. Cryst. Growth*, 2008, **310**, 2832–2841.
33 M. F. Butler, N. Glaser, A. C. Weaver, M. Kirkland and M. Heppenstall-Butler, *Cryst. Growth Des.*, 2006, **6**, 781–794.
34 C. Peng, Q. Zhao and C. Gao, *Colloids Surfaces A Physicochem. Eng. Asp.*, 2010, **353**, 132–139.
35 E. A. Chavez Panduro, T. Beuvier, M. Fernández Martínez, L. Hassani, B. Calvignac, F. Boury and A. Gibaud, *J. Appl. Crystallogr.*, 2012, **45**, 881–889.
36 F.C. Meldrum, H. Cölfen, *Chem. Rev.*, 2008, **108**, 4332–4432.
37 Y. Gao, S. Yu, X. Guo, *Langmuir*, 2006, **22**, 6125–6129.
38 P. Kašparová, M. Antonietti, H. Cölfen, Colloids Surfaces A Physicochem. Eng. Asp., 2004, **250**, 153–162.
39 H. Cölfen and M. Antonietti, *Langmuir*, 1998, **14**, 582–589.
40 J. Rudloff, M. Antonietti, H. Cölfen, J. Pretula, K. Kaluzynski, S. Penczek, *Macromol. Chem. Phys.*, 2002, **203**, 627–635.
41 M. Sedlak, M. Antonietti and H. Cölfen, *Macromol. Chem. Phys.*, 1998, **199**, 247–254.
42 K. Kaluzynski, J. Pretula, G. Lapienis, M. Basko, Z. Bartczak, A. Dworak, et al., *J. Polym. Sci. Part A Polym. Chem.* 2001, **39**, 955–963.
43 H. Cölfen, L. Qi, *Chem. A Eur. J.*, 2001, **7**, 106–116.
44 Q. Limin, L. Jie, M. Jiming, *Adv. Mater.*, 2002, **14**, 300–303.
45 T. Beuvier, B. Calvignac, G. J.-R. Delcroix, M. K. Tran, S. Kodjikian, N. Delorme, J.-F. Bardeau, A. Gibaud and F. Boury, *J. Mater. Chem.*, 2011, **21**, 9757–9761.
46 O. R. Davies, A. L. Lewis, M. J. Whitaker, H. Tai, K. M. Shakesheff and S. M. Howdle, *Adv. Drug Deliv. Rev.*, 2008, **60**, 373–387.
47 H. Tai, V. K. Popov, K. M. Shakesheff and S. M. Howdle, *Biochem. Soc. Trans.*, 2007, **35**, 516–521.
48 J. J. a Barry, M. M. C. G. Silva, V. K. Popov, K. M. Shakesheff and S. M. Howdle, *Philos. Trans. A. Math. Phys. Eng. Sci.*, 2006, **364**, 249–261.
49 M. Bhamidipati, A. M. Scurto and M. S. Detamore, *Tissue Eng. Part B. Rev.*, 2013, **19**, 221–232.
50 M. J. Cocero, Á. Martín, F. Mattea and S. Varona, *J. Supercrit. Fluids*, 2009, **47**, 546–555.
51 M.-K. Tran, A. Swed and F. Boury, *Eur. J. Pharm. Biopharm.*, 2012, **82**, 498–507.
52 A. I. Cooper, *J. Mater. Chem.*, 2000, **10**, 207–234.

53 B. Clément, B. Grignard, L. Koole, C. Jérôme and P. Lecomte, *Macromolecules*, 2012, **45**, 4476–4486.
54 J. Liu, Y. Pang, W. Huang, X. Zhai, X. Zhu, Y. Zhou and D. Yan, *Macromolecules*, 2010, **43**, 8416–8423.
55 W. Song, J. Du, N. Liu, S. Dou, J. Cheng and J. Wang, *Macromolecules*, 2008, **41**, 6935–6941.
56 Z. Zhao, J. Wang, H. Mao and K. W. Leong, *Adv. Drug Deliv. Rev.*, 2003, **55**, 483–499.
57 Y.-C. Wang, Y.-Y. Yuan, J.-Z. Du, X.-Z. Yang and J. Wang, *Macromol. Biosci.*, 2009, **9**, 1154–1164.
58 S. Wang, A C. Wan, X. Xu, S. Gao, H. Q. Mao, K. W. Leong and H. Yu, *Biomaterials*, 2001, **22**, 1157–1169.
59 M.-H. Xiong, Y. Bao, X.-Z. Yang, Y.-C. Wang, B. Sun and J. Wang, *J. Am. Chem. Soc.*, 2012, **134**, 4355–4362.
60 R. Dinarvand, F. Dorkoosh, M. Hamidi and S. H. Moghadam, *Biotechnol. Genet. Eng. Rev.*, 2004, **21**, 147–182.
61 Y.-C. Wang, X.-Q. Liu, T.-M. Sun, M.-H. Xiong and J. Wang, *J. Control. Release*, 2008, **128**, 32–40.
62 H. Vihola, A. Laukkanen, H. Tenhu and J. Hirvonen, *J. Pharm. Sci.*, 2008, **97**, 4783–4793.
63 Y. Li, F. Wang, T. Sun, J. Du, X. Yang and J. Wang, *Sci. China Chem.*, 2014, **57**, 579–585.
64 J. Wen, H.-Q. Mao, W. Li, K. Y. Lin and K. W. Leong, *J. Pharm. Sci.*, 2004, **93**, 2142–2157.
65 S. Monge, B. Canniccioni, A. Graillot and J.-J. Robin, *Biomacromolecules*, 2011, **12**, 1973–1982.
66 Q. Li, J. Wang, S. Shahani, D. D. N. Sun, B. Sharma, J. H. Elisseeff and K. W. Leong, *Biomaterials*, 2006, **27**, 1027–1034.
67 J.-J. Qiu, C.-M. Liu, F. Hu, X.-D. Guo and Q.-X. Zheng, *J. Appl. Polym. Sci.*, 2006, **102**, 3095–3101.
68 S. Zhang, H. Wang, Y. Shen, F. Zhang, K. Seetho, J. Zou, J. A. Taylor, A. P. Dove and K. L. Wooley, *Macromolecules*, 2013, **46**, 5141–5149.
69 S. Zhang, J. Zou, M. Elsabahy, A. Karwa, A. Li, D. a. Moore, R. B. Dorshow and K. L. Wooley, *Chem. Sci.*, 2013, **4**, 2122–2126.
70 S. Zhang, A. Li, J. Zou, L. Y. Lin and K. L. Wooley, *ACS Macro Lett.*, 2012, **1**, 328–333.
71 S. Zhang, J. Zou, F. Zhang, M. Elsabahy, S. E. Felder, J. Zhu, D. J. Pochan and K. L. Wooley, *J. Am. Chem. Soc.*, 2012, **134**, 18467–18474.
72 V. T. Huynh, G. Chen, P. de Souza and M. H. Stenzel, *Biomacromolecules*, 2011, **12**, 1738–1751.
73 R. Hoogenboom, *Angew. Chem. Int. Ed. Engl.*, 2010, **49**, 3415–3417.
74 R. C. Pratt, B. G. G. Lohmeijer, D. A. Long, P. N. P. Lundberg, A. P. Dove, H. Li, C. G. Wade, R. M. Waymouth and J. L. Hedrick, *Macromolecules*, 2006, **39**, 7863–7871.
75 F. Boury, J.-P. Benoit, O. Thomas and F. Tewes, *United States Pat.*, 2005, **US00836711**.
76 Y. Iwasaki and K. Akiyoshi, *Macromolecules*, 2004, **37**, 7637–7642.
77 Y. Iwasaki, S. Komatsu, T. Narita, K. Akiyoshi and K. Ishihara, *Macromol. Biosci.*, 2003, **3**, 238–242.
78 T.-M. Sun, J.-Z. Du, L.-F. Yan, H.-Q. Mao and J. Wang, *Biomaterials*, 2008, **29**, 4348–4355.
79 Y.-C. Wang, Y. Li, T.-M. Sun, M.-H. Xiong, J. Wu, Y.-Y. Yang and J. Wang, *Macromol. Rapid Commun.*, 2010, **31**, 1201–1206.
80 M. Xiong, J. Wu, Y. Wang, L. Li, X. Liu and G. Zhang, *Macrololecules*, 2009, **42**, 893–896.
81 S. Vanslambrouck, B. Clément, R. Riva, L.H. Koole, D. Molin, G. Broze, P. Lecomte, C. Jérôme, RSC Advances, 2015, **5**(35), 27330-37337.
82 M.-L. De Temmerman, J. Demeester, F. De Vos and S. C. De Smedt, *Biomacromolecules*, 2011, **12**, 1283–1289.
83 Y. Xiong, A. Steffen, K. Andreas, S. Müller, N. Sternberg, R. Georgieva and H. Bäumler, *Biomacromolecules*, 2012, **13**, 3292–3300.
84 G. B. Sukhorukov, D. V Volodkin, A. M. Gu and A. I. Petrov, *J.Mater. Chem.*, 2004, **14**, 2073–2081.
85 W. Hou and Q. Feng, *Mater. Sci. Eng. C*, 2006, **26**, 644–647.
86 C. Shivkumara, P. Singh, A. Gupta and M. S. Hegde, *Mater. Res. Bull.*, 2006, **41**, 1455–1460.
87 F. Manoli, J. Kanakis, P. Malkaj and E. Dalas, *J. Cryst. Growth*, 2002, **236**, 363–370.
88 T. Beuvier, B. Calvignac, J.-F. Bardeau, A. Bulou, F. Boury and A. Gibaud, *Anal. Chem.*, 2014, **86**, 9895–9900.
89 A. V. Radha and A. Navrotsky, *Rev. Mineral. Geochemistry*, 2013, **77**, 73–121.

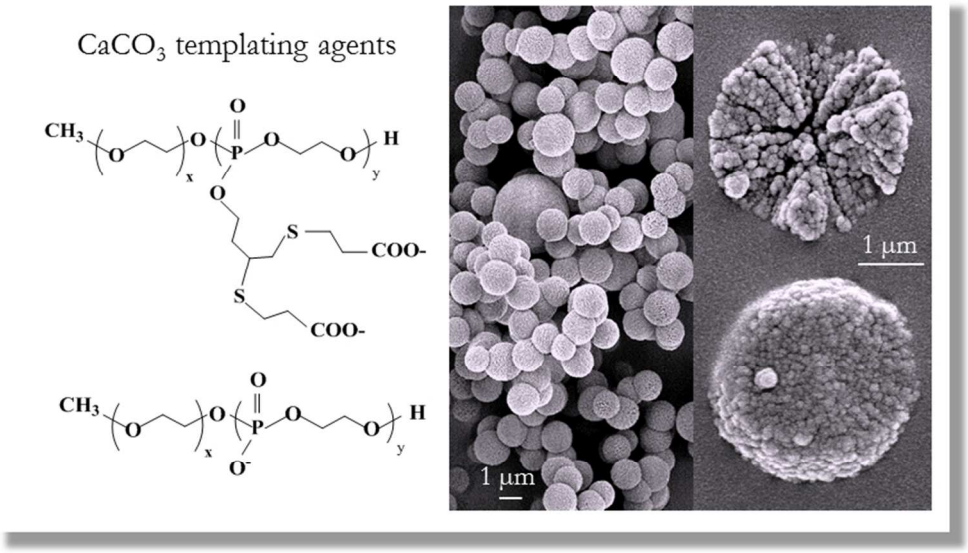

316x183mm (72 x 72 DPI)